JETIR.ORG ISSN: 2349-5162 | ESTD Year : 2014 | Monthly Issue
JOURNAL OF EMERGING TECHNOLOGIES AND INNOVATIVE RESEARCH (JETIR)
An International Scholarly Open Access, Peer-reviewed, Refereed Journal

DESIGN OF MICROWAVE PLANAR BANDPASS FILTER FOR APPLICATION IN WIRELESS COMMUNICATION

[1]Swathi G R, [3]Dr.Keerthi D S, [2] Dr. Murthi Mahadeva Naik G, [2]Dr. K C Deepika, [3]Dr. K B Santhosh Kumar

[1]Student, [2]Associate Professor, [3]Assistant Professor, [2]Associate Professor, [3]Dr. K B Santhosh Kumar

Electronics and Communication,
Malnad College of Engineering, Hassan-Karnataka, India

Abstract: The purpose of a numerous effective methods for Spectrum provisioning control, Spectrum congestion is emerged as a significant problem. Ceiling popular frequencies, which are 700-megahertz frequency band to 3,000 megahertz and 2,400 megahertz to 6 GHz, interference is inevitably increasing in direct proportion to the number of emitters. A very compact four notches bandpass filter utilizing rectangular ring resonator structure with novel method to generate an ultra-wideband (UWB) bandpass filter (BPF). Initially, this method employs a stub-loaded rectangular ring resonator (SLRRR) based compact structure to develop a UWB bandpass filter. The compact sized (24.35x31.7 mm^2) and Ground Plane with size 2.4 mm^2 of X-axis,7.2 mm^2 of Y-axis proposed filter is characterized by a wide passband extending from 3.3to 9.1GHz with low insertion loss of < -0.65 dB The operating mid correspond fractional Bandwidth is 80%, respectively. Structures are fabricated, measured, and compared with the obtained simulation outcomes. The resemblance between the compared results corroborates the applicability of such compact structure and developed based on the analysis.

Keywords-UWB bandpass filter, insertion loss, SLRRR, Compact size.

.

I. INTRODUCTION

Researchers have been paying more and more attention to the ultra-wideband technology area ever since the FCC designated the ultra-wide frequency band (3.1–10.6GHz) as the operational band for commercial devices without licenses. The fundamental multi-layer structure of microstrip-slot wire-microstrip wide edge coupling serves as the foundation for the creation of the three types of filters. Three-class connections are used to achieve the ultra-wideband filter. The double broadband filter is intended to be realized through the intermediate coupling layer of the multimode resonator and coplanar waveguide. By altering the middle coupling slot structure and employing a curved T SIR construction, the ultra-wideband filter is achieved [1].

It is suggested to use a linked step-impedance resonator bandpass filter. The filter is a dual-band switchable and tune able band-pass filter for Bluetooth and 5G NR applications. It combines U-shaped and L-shaped branches to create multiple resonance points while expanding the bandwidth. Additionally, the folded structure improves the in-band ripple and significantly reduces the filter size [2]. The filter uses separate switching and tuning techniques made possible by PIN and varactor diodes, operating at 2.41GHz for Bluetooth and 3.55GHz for 5G. With compact dimensions of $0.177\lambda g \times 0.096\lambda g$, a minimum insertion loss of 0.35dB, and a significant return loss of 30dB [3], the proposed design features a triple-band bandpass filter based on fractal geometry and metamaterials [4]. One benefit of the suggested stepped-impedance stub-loaded resonator (SISLR) is that it offers additional degrees of freedom for adjusting the resonant frequency [5].

The asymmetric arrangement of the rectangular ring resonator structure in relation to two parallel signal flow routes connected to input/output ports has been investigated in this article. To design UWB BPF, a unique stepped-impedance stub-loaded ring resonator (SISLR) is suggested. According to an analysis of the suggested ring resonator's features, the necessary resonant modes can be conveniently moved within the UWB band because it has more degrees of adjustment freedom to manipulate its resonant frequencies.

II. LITERATURE SURVEY

[1]. The UWB filter passband from 2.90 to 10.90 GHz against the counterpart frequency of 2.92 to 10.72 GHz in simulation. The measured return loss is lower than 10 dB within most part. The overall dimensions of are around 0.73 λ_0 X 0.35λ_0. "Design concerning a UWB bandpass filter with stepped-impedance stub loading Resonator" (2010).

[2]. Comparison where proposed filter design characteristics are dielectric constant 2.55/0.8, S.F (0.921), 3dB FBW 117%, Size (0.514x0.312). "Novel UWB Bandpass Filter Using Stub-Loaded Multiple-Mode Resonator" (2011)

[3]. Compared with other recent MMR based UWB bandpass filters *εr/t* (mm) 2.5/0.8(εr/t(mm)),0-0.5 (IL (dB)), 12(RL (dB)), 6.14/>16(USB (GHz)/ Attenuation(dB)),0.21-0.35(GD (ns)), 22.5×14 Size (mm2), 111.6 FBW, S.F(0.9).” Compact Setting Up an Open-Ended stub loaded multi-mode Resonator-Based High selectivity UWB Bandpass filter “(2021).

[4]. Comparison was proposed filter design characteristics are *εr/t* (mm) 2.5/0.8, IL (dB) 0.3–0.97, USB (GHz)/ Attenuation (dB) 5.37/20, No of notches (3), Notch frequency (GHz)/ attenuation (dB) 6/16.16, 6.53/26.47, 8.35/15.22, Size ($\lambda g \times \lambda g$) 0.81 × 0.71. “Highly Selective Comb-Shaped UWB Bandpass Filter with Multi-Notch Features Resonator” (2022).

[5]. Comparison where proposed filter design characteristics are Center freq. (GHz) 0.94/2.48, IL (dB) 0.28/0.92, 3-dB FBW (%) 39/27, TZs 6, size (*λg× λg) 0.12X0.1*. “Design of a planar Compact Dual-Band Using a Bandpass filter with Several Transmission Zeros a Stub-Loaded Structure” (2023).

[6]. Comparison where proposed filter design characteristics are Passbands (GHz) 3.3/5.7, Passband BW (Wide/Narrow), FBW% (72/2.6), Independent, controlled passband (YES), Size *λg* λg (0.58x0.122).* “Multi-Band Band-Pass Filter with Independently Controlled Asymmetric Dual-Band Response Based on Meta cell” (2024).

[7]. Comparison where proposed filter design characteristics are Frequency range (GHz) (2.4–3.5), Insertion loss (dB) 3.5, Return loss (dB) 25, Dimensions $\lambda g * \lambda g$ (0.17 × 0.09), Rejection level (dB) 35. “Switchable/Tenable Dual-Band BPF for Bluetooth and 5G NR Applications” (2025).

[8]. Comparison where proposed filter design characteristics are Overall size $\lambda g \times \lambda g$ (0.85 × 0.54), Frequency (GHz) 11/6/5, Insertion loss (dB) 0.26/1/0.39, Type Triple Band, Fabrication (Yes).

“Design of a Triple-Band Metamaterial Bandpass Filter Utilizing Modified-Minkowski Fractal Geometry” (2025).

[9]. Comparison where proposed filter design characteristics are Center Frequency (GHz) 54, Fractional Band widths 57.7%, Insertion Loss (dB) 1.5, Size (mm3) 36×22×1.218. “Filter Design Based on Multilayer Wide Side Coupling Structure” (2024).

[10]. Comparison where proposed filter design characteristics are Filter size (mm2)9.6 × 8.8, FBW 60.2%, IL (dB) < 1.1, RL (dB) > 13. “Bandpass Filter for 5G Sub-6 GHz Bands” (2024).

[11]. Comparison where proposed filter design characteristics are *f*0 (GHz)2.43, IL (dB) 0.9, Stopband width 8.2*f*0 (> 18 dB), Size ($\lambda g \times \lambda g$) 0.23 × 0.33. “Design of a Novel Miniaturized Wide Stopband Filtering Coupler” (2023).

[12]. Comparison where proposed filter design characteristics are Freq (GHz) 2.8, Sensitivity (%) 2.342, Relative size (λ 2 *g*) 1.13λg × 1.13λg, Cover range (*εr*) 1–25, Non-contact (Yes).” Antenna Sensor Based on an Inter-Digital Capacitor Shape EBG Structure for Liquid Dielectric Measurement (2024).

III. Design of Proposed UWB BPF

By identifying the proposed design as a series of cascaded two-port networks and characterizing it using an ABCD matrix, the rectangular ring allowed for the production of three notches at 4.62, 7.11, and 9.49 GHz, respectively, with a horizontally and vertically asymmetric layout and a simple design. The overall equivalent circuit is therefore determined by the matrix product of multiple ABCD matrices of the cascaded two-port networks. In this regard, it should be mentioned that the ring resonators that have been developed in previous studies have a structural form that is vertically symmetric. However, a rectangular ring resonator structure with horizontal symmetry achieves the first ultra-wide passband realization.

Parallel signal flow transmission lines are highly regarded for a strong coupling between the ring and the ports, in addition to the single coupled line connected to the entry and the single coupled line connected to a parallel rectangular ring. Thus, this tiny design has accomplished four notches without any structural complication by employing the asymmetric layout that goes along with parallel signal transmission pathways. The HFSSV13 software is used to develop and simulate UWB filters. Arlon, a substrate material with a dielectric loss tangent of 0.0015 and a relative dielectric constant of 2.5, is chosen to be 0.8 mm thick.

For a tight coupling between the ring and the ports, parallel signal flow transmission lines are crucial. In addition to the single coupled line attached to the entrance, the single coupled line is also connected to a parallel rectangular ring. Without any structural complication, this tiny design has accomplished four notches by leveraging the asymmetric layout that goes along with parallel signal transmission pathways. Using HFSSV13 software, UWB filter design and simulation are carried out. The substrate material is Arlon, which is 0.8 mm thick and has a dielectric loss tangent of 0.0015 and a relative dielectric constant of 2.5.

a=3, b=3, c=8.1, d=1.2, e=0.4, f=0.21, g=8.9, k=1.72, l=2.4, m=0.4, n=11.5, 0=0.26, p=3, q=1.2, r=0.4, s=0.64, t=7.2, u=8.1, v=3.21, W=24.35, x=8.16, y=0.24, Z=12.4, L=31.7

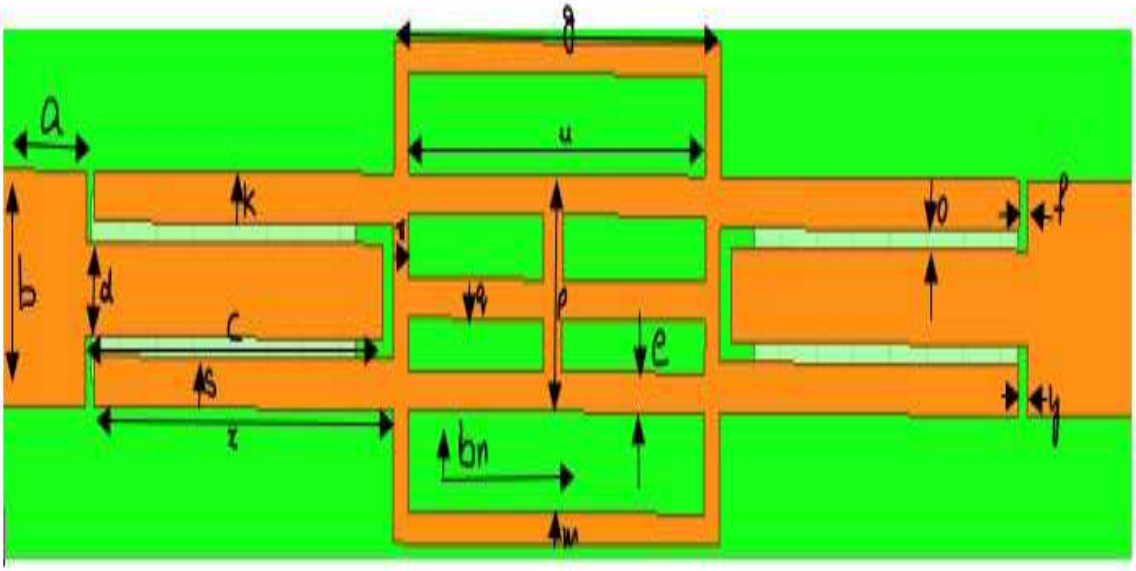

Fig.1(a) Structural views of the proposed UWB bandpass filter-Front view

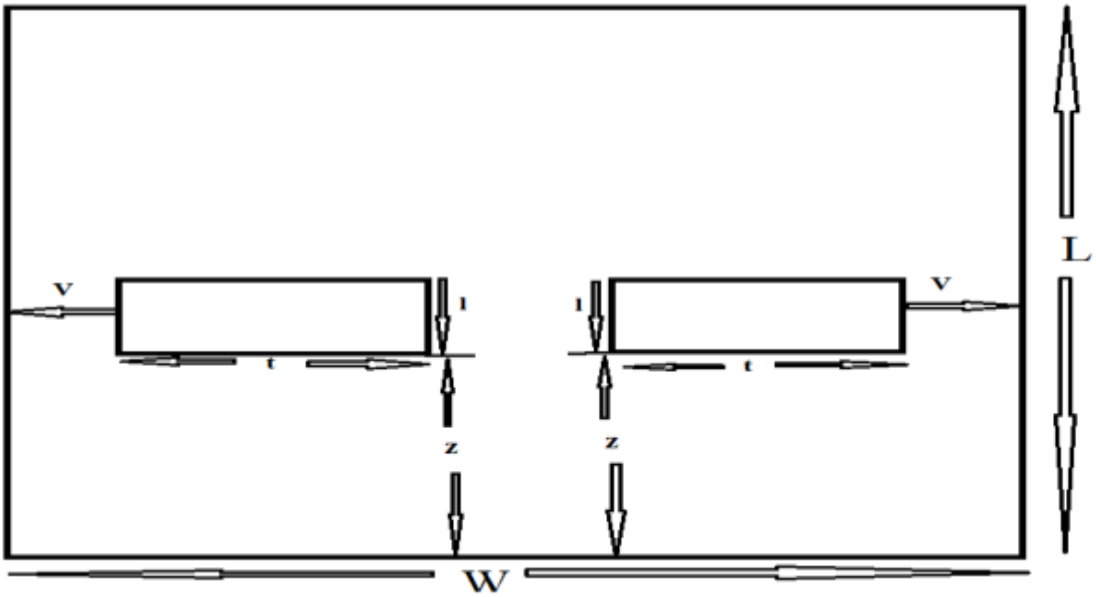

Fig.1(b) Structural views of the proposed UWB bandpass filter- Rear view.

IV. RESEARCH METHODOLOGY

It is evident that the simulated outcomes closely match the design objectives. The discontinuity impact of the micro strip lines may be the cause of slight frequency variations. As previously mentioned, UWB passband can be created if this SLARRR is appropriately fed with two interdigital parallel-coupled lines with a higher coupling degree.

Strong coupling agreement between the ports and the ring is required to achieve stable pass band transmission properties. Figure 2(a) shows |S21| characteristic curves for various coupling values, which enable a slow change from week to strong coupling.

The structure produces three resonant peaks at frequencies f1=4.62GHz, f2=7.11GHz, and f3=9.49GHz when the minimum coupling is permitted. The insertion losses are gradually overcome by a moderate increase in the length of a single couple of lines, which is ultimately tuned at -0. 65 dB.

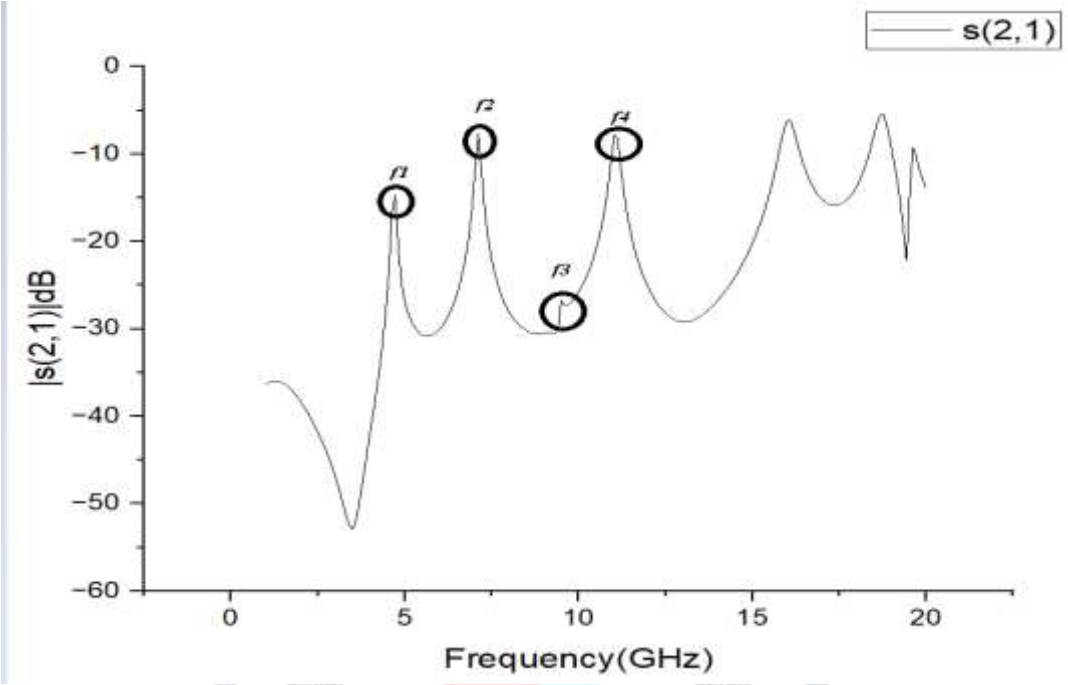

Figure 2 (a). shows |S21| characteristic curves for various coupling values

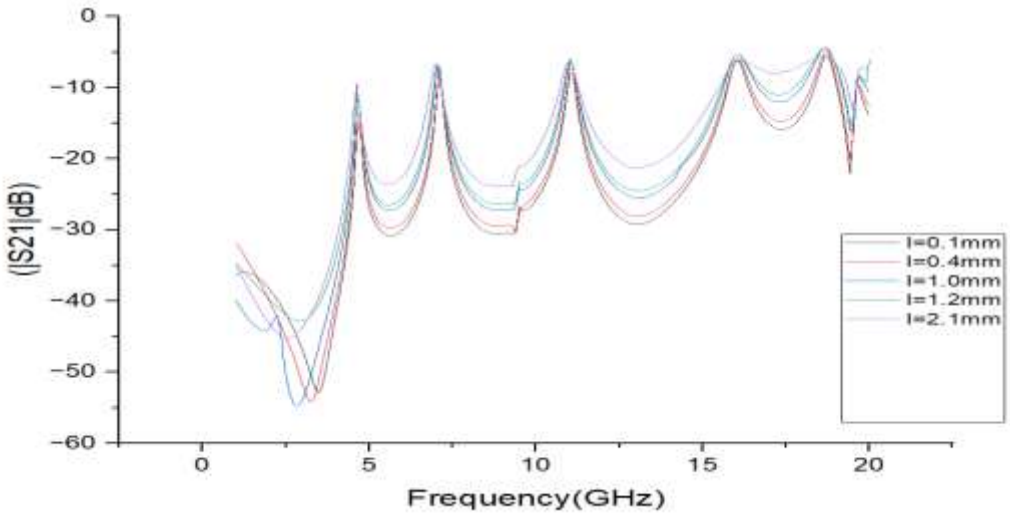

Figure 2 (a) & (b). The magnitude of |S21| under weak coupling conditions

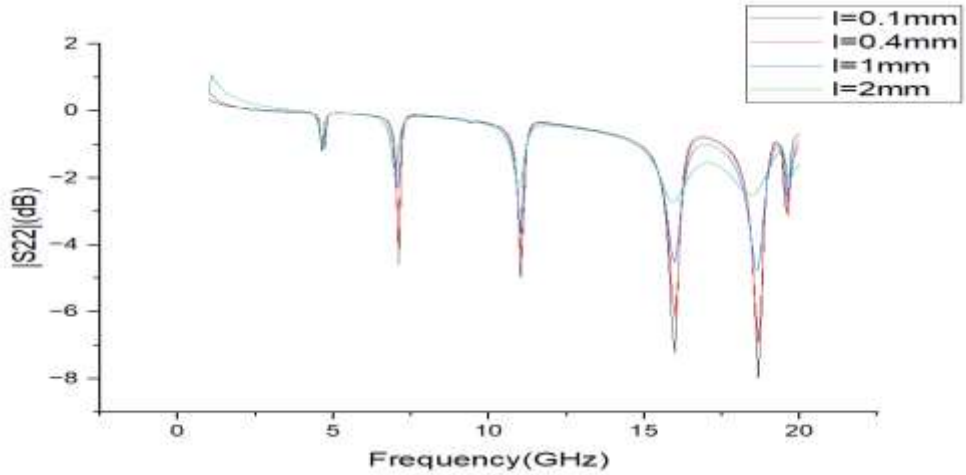

Figure 2(c). The magnitude of |S22| under weak coupling conditions

Next, Figure 3 justifies the important role of the aperture, which is positioned at the rear of the substrate in a suitable manner for a superior performance display. It is evident that the lack of an aperture significantly impairs the impedance matching process, which leads to a significant decline in the filter's output response because of excessive insertion loss.

The ground plane apertures have a significant impact on the UWB bandpass filter's effectiveness as well. The filter performance is examined in Fig. 4 both with and without the ground plane apertures. It is evident from the curve patterns of both |S11| and |S21| that the impedance matching of the filter design is significantly hampered in the absence of the aperture. This occurs because, in the absence of ground plane apertures, there is a maximum coupling between the arms of interdigital lines and the ground plane.

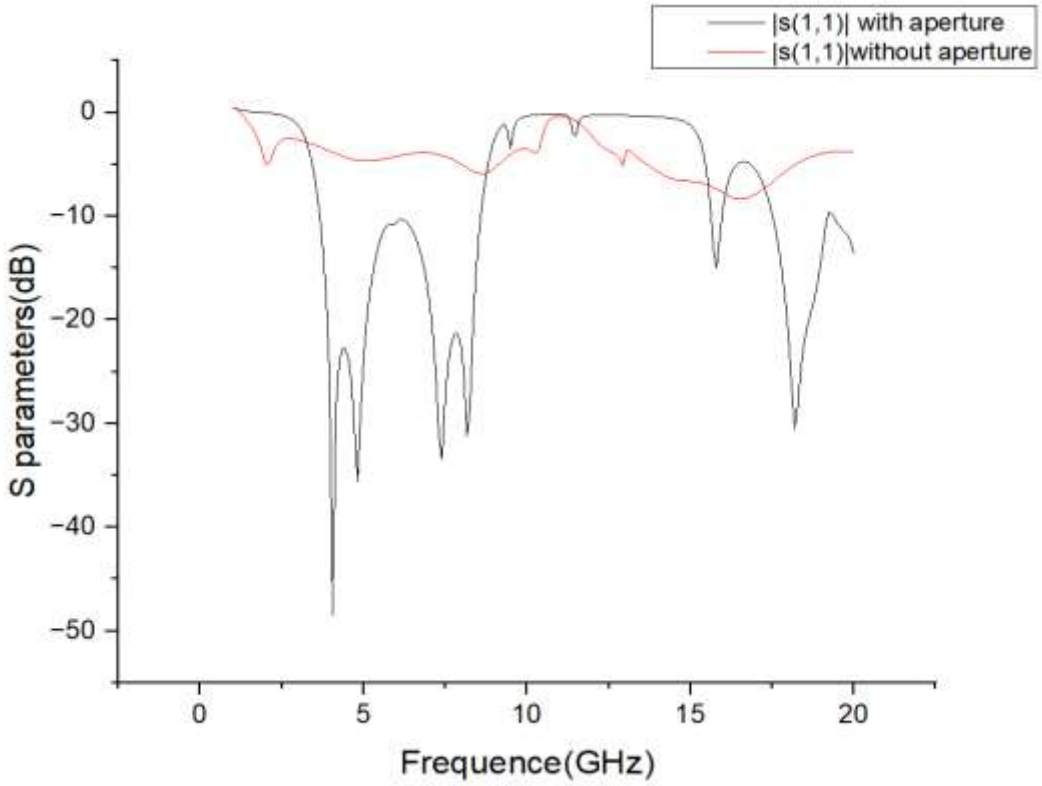

Fig. 3(a) Simulated S-parameter response in presence and absence of the ground plane apertures -Variation of |S11|

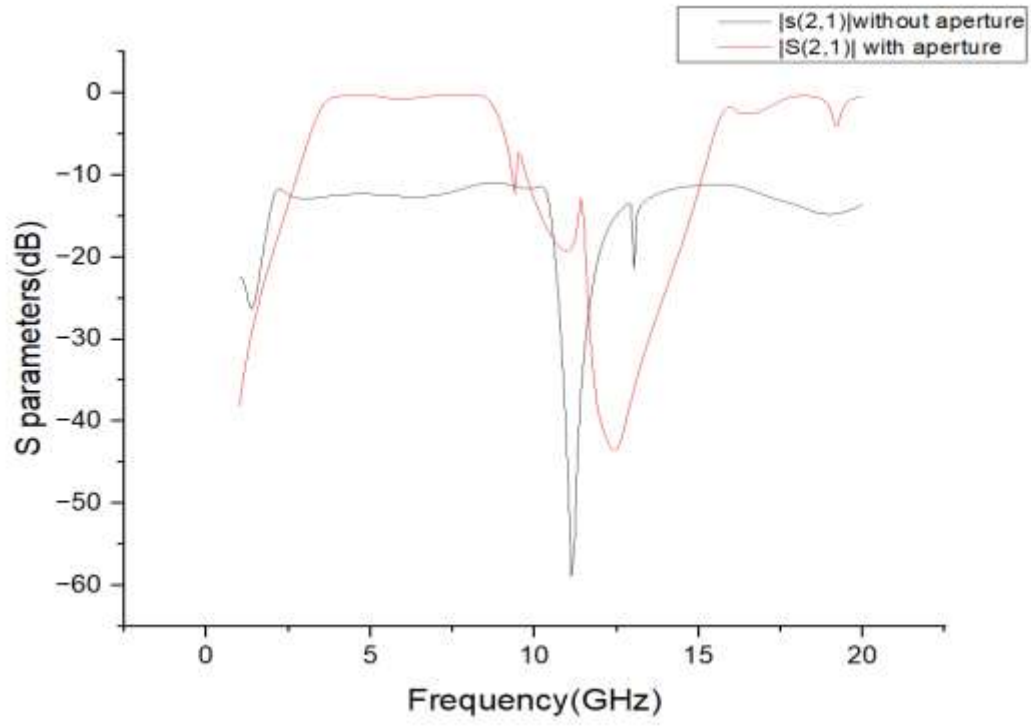

Fig. 3(b) Simulated S-parameter response in presence and absence of the ground plane apertures -Variation of |S21|

Lastly, Fig. 4 shows the suggested filter's overall performance. The S parameters plots under the “with aperture” condition in Figure 3(a) ultimately have encapsulated all the passband achieved by the proposed notched band bandpass filter succinctly. Over the filter's operational bandwidth, the |S11|- variation is found to be better than -12 dB Less than -0.5 dB is the uniform and extremely low insertion loss of the suggested filter. Higher frequency selectivity for the filter and a smooth transition between the stopband and the passband are made possible by the presence of two transmission zeros at 2.45 GHz and 10.51 GHz with attenuation levels of -48.44 dB and -29.71 dB, respectively. As seen in Fig. 4(b), the group delay curve fluctuates between 0.2 and 0.3 ns and is almost

flat over the passband. The filter's overall dimensions are 24.35 x 31.7 mm2, which is significantly smaller than the stated bandpass filter.

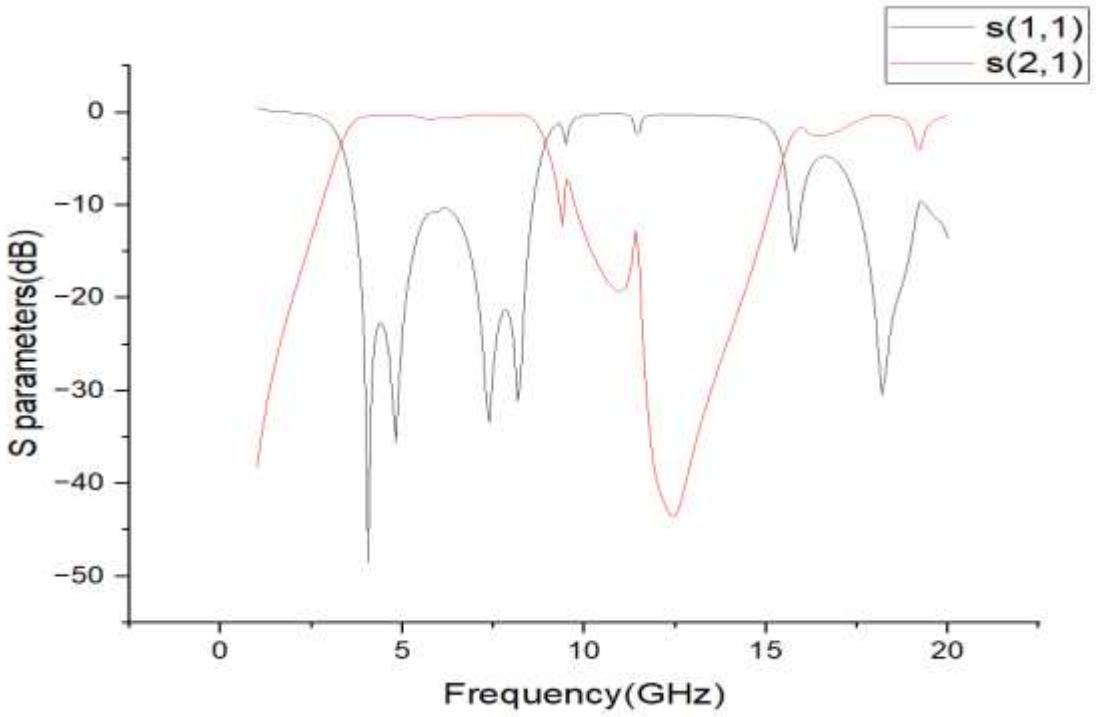

Fig. 4 (a) Simulation outcome of the proposed UWB bandpass filter- S parameter response

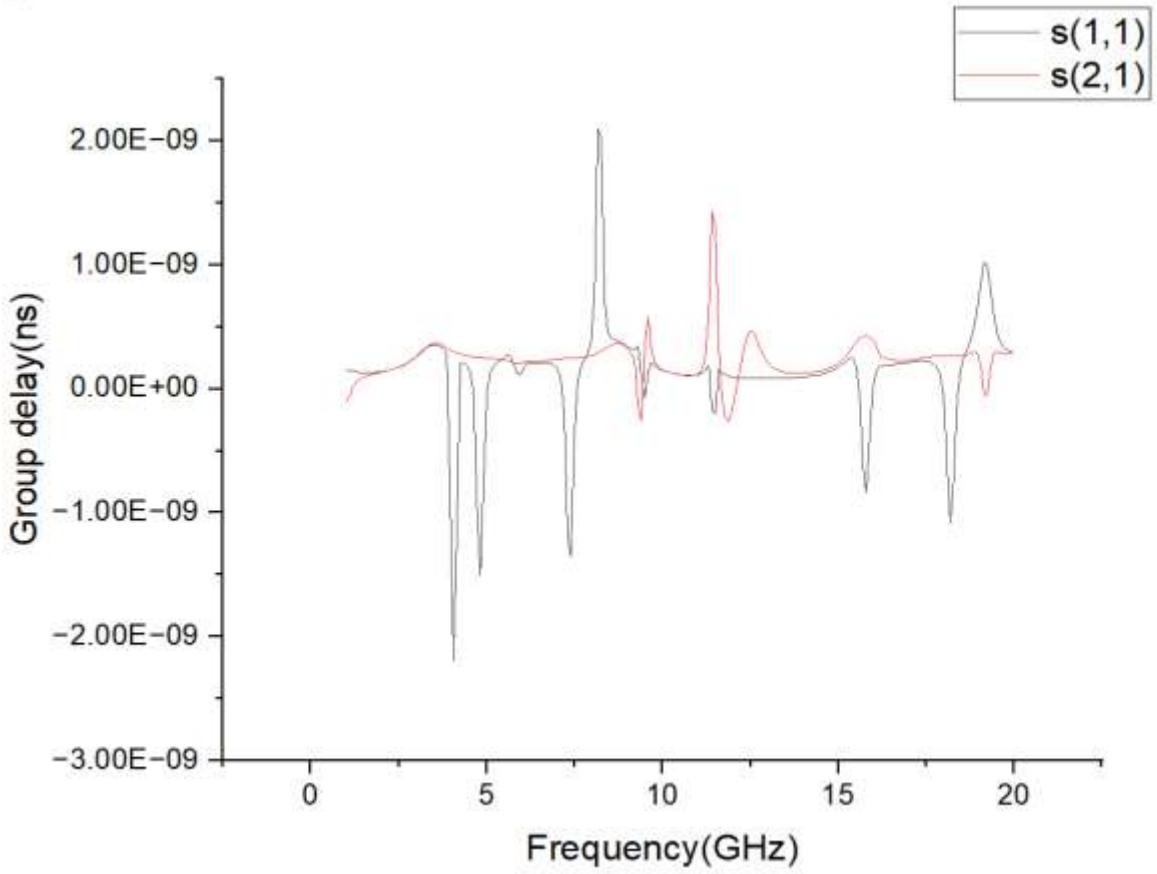

Fig. 4(b) Simulation outcome of the proposed UWB bandpass filter -Group delay.

V. RESULTS AND DISCUSSION

4.1 Results of Descriptive Statics

Table 4.1: PERFORMANCE COMPARISON WITH PUBLISHED FILTER DESIGNS

Ref	Size(mm2)	IL(Db)	FBW%
[1]	36x22x1.218	1.5	57.7
[5]	9.6x8.8	1.1	60.2
[6]	0.17x0.09(λg)	3.5	37.2
[7]	0.85x0.54(λg)	0.26	58.8
[8]	22.5x14	0.5	111.6
[*]	24.35x31.7	0.65	80

Table 4.1 The suggested filter properties are contrasted with Bandpass filters for ultra-wideband found in the comparison table. Filter size in mm^2, percentage of 3 dB passband fractional bandwidth, insertion and return loss in dB, and substrate dielectric constant and thickness in mm2 are all represented by column-wise entries in this case. When compared to other contemporary filters that are accessible in the literature, it is evident from the comparison table that the suggested filter has simultaneously attained a broad passband FBW of 80%.

Finally, A novel technique for parallel-coupled filter modification with a new asymmetrical design strategy to create a miniature UWB band pass filter. By creating three distinct frequency bands with notches of 4.72 GHz, 7.11 GHz, and 9.49 GHz Characterized by narrow FBWs of 80% each, the suggested solution, which is appropriate for moderate to wide bandwidth filter realization with the SLARRR model.

Additionally, the design has been considered suitable for UWB applications due to its other attributes, such as an acceptable reflection coefficient, low insertion loss of −0.65dB, good selectivity of 0.8 at −20dB, compact dimensions (24.35x31.7 mm^2), and strong correlation between simulated and measured results. The inline Input and result with the filter's main axis may make the suggested filter design approach beneficial. This is because circuit design with extremely tight space limitations, imposed by the ever-desired circuit downsizing, might benefit from this feature. In summary, the suggested filter's tiny size, straightforward design, and excellent in-band and out-of-band performance are all demonstrated.

References

[1]. Partha Pratim Shome, Arindam Deb, Anirban Neogi, Jyoti Ranjan Panda (2021) was proposed “Compact Configuration of Open-Ended Stub Loaded Multi-Mode Resonator Based UWB Bandpass Filter with High Selectivity “2021 8th International Conference on Signal Processing and Integrated Network (SPIN).
[2]. Guang Yong Wei1, Yun Xiu Wang1, *, Jie Liu1, 2, and Hai Ping Li1 (2023) “Design of a Planar Compact Dual-Band Bandpass Filter with Multiple Transmission Zeros Using a Stub-Loaded Structure” Progress in Electromagnetics Research letter, Vol.109, 23-30, 2023.
[3]. Partha P. Shome2, Jyoti R. Panda1, and Arindam Deb, Piali Chakraborty (2022) “Highly Selective UWB Bandpass Filter with Multi-Notch Characteristics Using Comb Shaped Resonator” Progress in Electromagnetics Research M, Vol.108, 89-101, 2022.
[4]. Shobha Hugar1, *, Jambunath Baligar2, Veerendra Dakulagi3 , and K. M. Vanitha (2024) “Multi-Band Band-Pass Filter with Independently Controlled Asymmetric Dual-Band Response Based on Meta cell” Progress in Electromagnetics Research letter, Vol.122, 81-86, 2024.
[5]. Areeg F. Hussein1, *, Malik Jasim Farhan1, and Jawad K. Ali (2025) “Switchable/Tunable Dual-Band BPF for Bluetooth and 5G NR Applications” Progress in Electromagnetics Research C, Vol.152, 103-110, 2025.
[6]. Hayder S. Ahmed∗ and Aqiel N. Almamori (2025) “Design of a Triple-Band Metamaterial Bandpass Filter Utilizing Modified-Minkowski Fractal Geometry” Progress in Electromagnetics Research C, Vol.154, 159-167, 2025.
[7]. Wusheng Ji1, 2, Hanglin Du1, 2, *, Yingyun Tong1, 2, Xiaochun Ji1, 2, and Liying Feng (2024) “Filter Design Based on Multilayer Wide Side Coupling Structure” Progress in Electromagnetics Research M, Vol.128, 31-39, 2024.
[8]. Jiajia Wang1 , Shuo Yu1 , Xiaofan Yang2 , and Xiaoming Liu(2024) “Bandpass Filter for 5G Sub-6 GHz Bands” Progress in Electromagnetics Research C, Vol.152, 103-110, 2024.
[9]. Xiaming Mo1 , Yongkang Yuan1 , Minquan Li1, *, Pingjuan Zhang2 , Yajing Yan1 , Guangxiu Zhao1 , and Ziyun Tu (2023) “Design of a Novel Miniaturized Wide Stopband Filtering Coupler” Progress in Electromagnetics Research M, Vol.119, 105-116, 2025.
[10]. Bo Yin and Juntao Yin(2024) “Antenna Sensor Based on an Inter-Digital Capacitor Shape EBG Structure for Liquid Dielectric Measurement” Progress in Electromagnetics Research C, Vol.140, 65-73, 2024.
[11]. Xiaming Mo1 , Yongkang Yuan1 , Minquan Li1, *, Pingjuan Zhang2 , Yajing Yan1 , Guangxiu Zhao1 , and Ziyun Tu (2023) “Design of a Novel Miniaturized Wide Stopband Filtering Coupler” Progress in Electromagnetics Research M, Vol.119, 105-116, 2025.
[12]. Bo Yin and Juntao Yin(2024) “Antenna Sensor Based on an Inter-Digital Capacitor Shape EBG Structure for Liquid Dielectric Measurement” Progress in Electromagnetics Research C, Vol.140, 65- 73, 2024.